Supporting Information

Boosting Sodium Storage in TiO2 via Synchronous Surface Sulfurization and Amorphization

Meinan Zhao,[a] Bing Yu,[a] Peiyao Wang,[b] Xiao Li,[e] Shendong Xu,*[c] Yun Song,[d] and Yongtao Li*[a]

a. Key Laboratory of Efficient Conversion and Solid-state Storage of Hydrogen & Electricity of Anhui Province, School of Materials Science and Engineering, Anhui University of Technology, Maanshan 243002, China. E-mail: liyongtao@ahut.edu.cn

b. Key Laboratory of Materials Physics, Institute of Solid State Physics, HFIPS, Chinese Academy of Sciences, Hefei 230031, China. E-mail: pywang@issp.ac.cn

c. School of Carbon Neutrality Science and Engineering, Anhui University of Science and Technology, Hefei 231131, China. E-mail: 2024226@aust.edu.cn

d. College of Smart Materials and Future Energy, Fudan University, Shanghai, 200433, China. E-mail: songyun@fudan.edu.cn

e. Hefei General Machinery Research Institute Co., Ltd, Hefei 230031, China. E-mail: lixiao_hgmri@163.com

Experimental

Preparation of S-TiO_2 powder

S-TiO_2 powder was prepared via a one-step gas-phase vulcanization method. Typically, 100 mg of TiO_2 powder and 120 mg of sulfur powder were placed in a tube furnace. The sample was then heated at 550 °C for 2 hours under a continuous argon flow, resulting in a light-yellow powder denoted as S- TiO_2. For comparison, a sample treated for 5 hours under identical conditions was also prepared. A simple preparation diagram is shown in Figure 2a. However, the obvious agglomeration and grain growth were observed in the black powder after vulcanization for 5h by transmission electron microscopy. (as shown in Figure S1), this will seriously affect its electrochemical performance, therefore, the key research object of this experiment is TiO_2 which was vulcanized for 2 h.

Structural characterization of materials

Scanning electron microscope characterization was performed on JSM-6490, transmission electron microscope characterization was carried out on JSM-2000, the UV-Vis absorption spectrum was analyzed by Lambda 25 UV-Vis spectrophotometer. The structure and phase composition of the material were characterized by powder X ray diffractometer(XRD，D8-ADVANCE，Bruker). X-ray photoelectron spectroscopy (XPS，Thermo Fisher Scientific K-Alpha) was used to analyze the chemical composition and valence state of materials under the vacuum of $2x10^{-9}$ mbar through monochromatic Al and Kα X-ray sources.

Characterization of electrochemical performance

The quality of electrode sheet is measured by fully automatic electronic analytical balance (Quintix 35-1CN, Sartorius). S-TiO_2 was used as negative electrode (among them, graphene was used as conductive agent, PVDF as binder, and the mass ratio of active substance, conductive agent and binder is 7:2:1). The typical areal mass loading of the active material (S- TiO_2 or TiO_2) was ~1.2–1.5 mg cm^{-2}. High purity sodium metal was used as counter electrode, polypropylene microporous membrane (Celgard 2400) was used as the diaphragm, 1mol L^{-1} $NaClO_4$ EC:DMC(1:1) was used as electrolyte for sodium battery and assembled into 2032 button type battery. The whole battery assembly process was carried out in an argon glove box. ($O_2 < 0.1$ ppm; $H_2O <$ 0.1 ppm) Both the cyclic voltammetry test and the AC impedance test were carried out on the electrochemical workstation with the Solartron Mobrey England SI1287 test system. Constant current charge-discharge test was carried out in Xinwei electrochemical test system. All samples were measured at ambient temperature(25 C°) . Considering that the theoretical specific capacity of anatase TiO_2 is 335 mAh g^{-1}, therefore, we will apply the current density 335 mA g^{-1} as the 1 C in charge discharge rate.

Computational details

All of calculations were performed via Vienna *ab initio* simulation package (VASP) by using the first principles based on DFT. The generalized gradient approximation

(GGA) potential of Perdew-Burke-Ernzerhof (PBE) was used in relaxation. The projector augmented wave (PAW) method was applied to describe the pseudopotential. The lattice parameters and nuclear coordinates derived from the anatase TiO_2 (I_{41}/amdz). The electronic configurations of Ti, O, S, and Na are $[Ar]3d^24s^2$, $2s^22p^4$, $3s^23p^4$, and $2p^63s^1$, respectively. 1×1×1 unit cells of TiO_2 and S-TiO_2 is employed to study their structural and electronic properties. The energy cutoff is set to 500 eV for all cases, and gamma-centered meshes with 5×5×2 *k*-points for simulate all models, in reciprocal space were used during geometric optimization. The convergence tolerance is 0.01 eV/Å for the force on atom and the energy difference between two continuous ionic steps is less than 10^{-5} eV. The formation energy of S-TiO_2 is defined as:

$$E_{f}=[E_{(S-TiO_2)}-N1E_{(Ti)}-N2E_{(O)}-N3E_{(S)}]/N1+N2+N3 \qquad (1)$$

$E_{(S-TiO_2)}$, $E_{(Ti)}$, $E_{(O)}$, and $E_{(S)}$ are the total energy of S-TiO_2, one Ti in bulk states, O and S in ground states, respectively. N1, N2, and N3 are the number of Ti and O atoms in TiO_2, respectively. The capacity can be obtained via following equation:

$$C=xF/M_{S-TiO_2} \qquad (2)$$

here, x represents the number of electrons in the electrochemical process, F is the Faraday constant (26.8 Ah mol^{-1}), and M_{S-TiO_2} is the mass of S-TiO_2.

Table S1. The fitted EIS results from the equivalent circuits.

	R_e(ohm)	**Error(%)**	**R_{ct}(ohm)**	**Error(%)**
S-TiO_2	109.2	1.204%	221.9	1.845%
TiO_2	93.46	0.759%	385.2	0.857%

Table S2. Structural parameters and phase abundance of the TiO_2 and S-TiO_2 obtained by Rietveld analysis on XRD patterns.

Sample	**Structure type**	**Space Group**	**Lattice Parameters(Å)**		**S**	**Abundance**
			a	**c**		**(wt.%)**
TiO_2	anatase	*$I4_1/amd$*	3.7907(1)	9.5209(3)	2.9	95
	rutile	*$P4_2/mnm$*	4.6085(2)	2.9627(2)		5
S-TiO_2	anatase	*$I4_1/amd$*	3.7904(2)	9.5203(8)	2.8	94
	rutile	*$P4_2/mnm$*	4.6096(3)	2.9614(5)		6

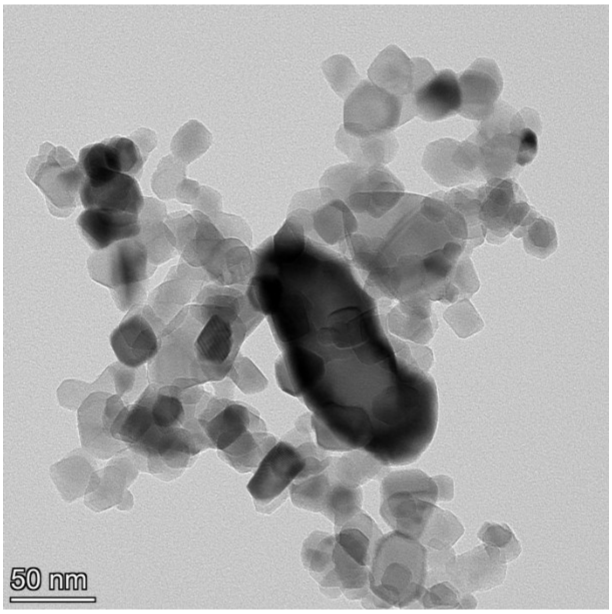

Fig. S1 HRTEM image of TiO_2 vulcanized for 5 hours.

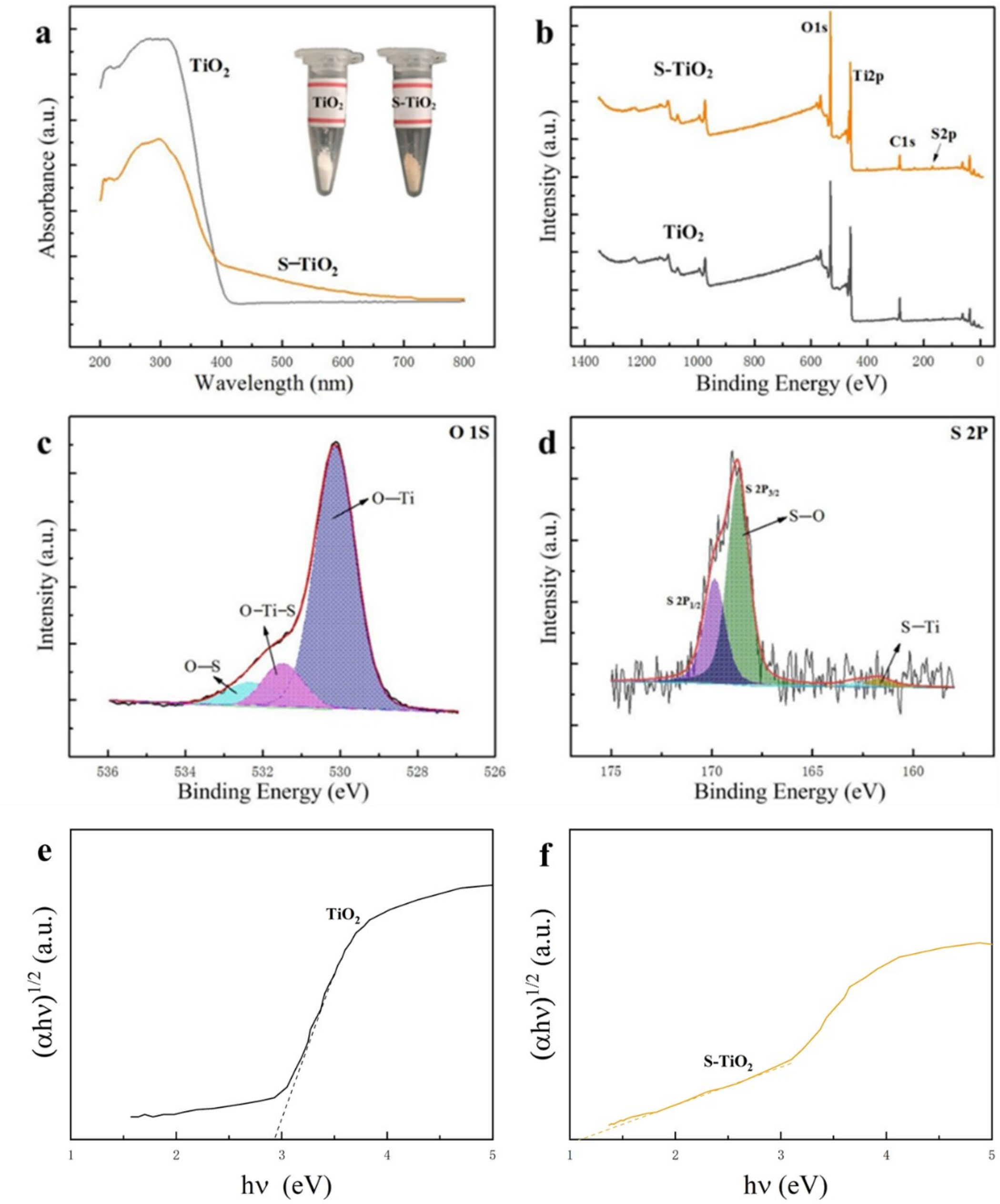

Fig. S2 Spectra analysis of S-TiO_2 samples: (a) Ultraviolet-visible absorption spectrum, (b) Full spectrum analysis of X-ray photoelectron spectroscopy, (c) High resolution spectrum of O element, (d) High resolution spectrum of S element, (e) Tauc plot for pristine TiO_2, (f) Tauc plot for S-TiO_2.

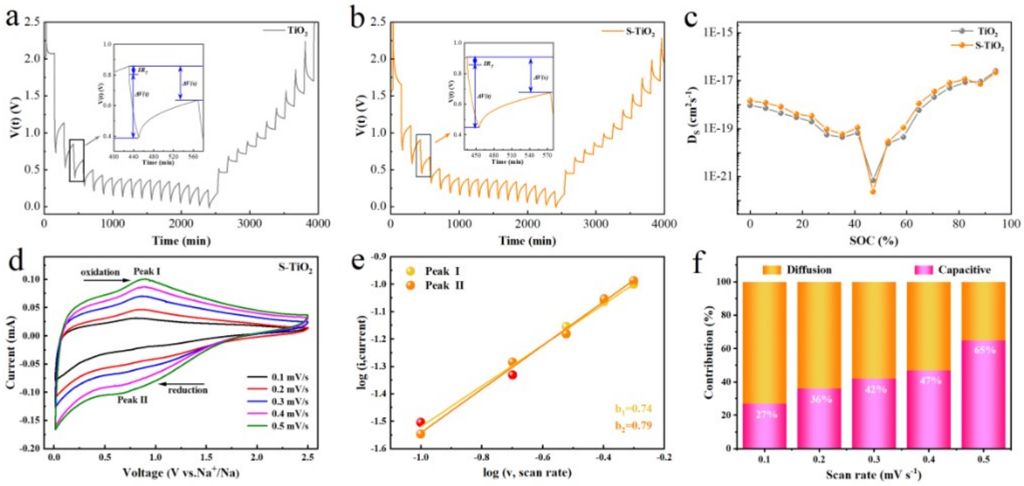

Fig. S3 Study on the kinetic properties of S-TiO$_2$ electrode materials:(a-c) GITT data for TiO$_2$ coin cell and S-TiO$_2$ coin cell, diagram of voltage versus time(a)TiO$_2$, (b)S-TiO$_2$, the illustrations in (a) and (b) are correspond to zoomed-in voltage, (c) measured diffusivities D$_s$ versus SOC for GITT, (d-f) Analysis of Pseudo-Capacitance behavior of S-TiO$_2$, (d) Cyclic voltammetric curves of S-TiO$_2$ at different scanning rates(0.1 to 0.5 mV s^{-1}), (e) Curve of lg$\boldsymbol{i}$ vs lg$\boldsymbol{v}$ at different peak voltages, (f) Bar graph of the proportion of pseudocapacitance contribution at different scanning rates.

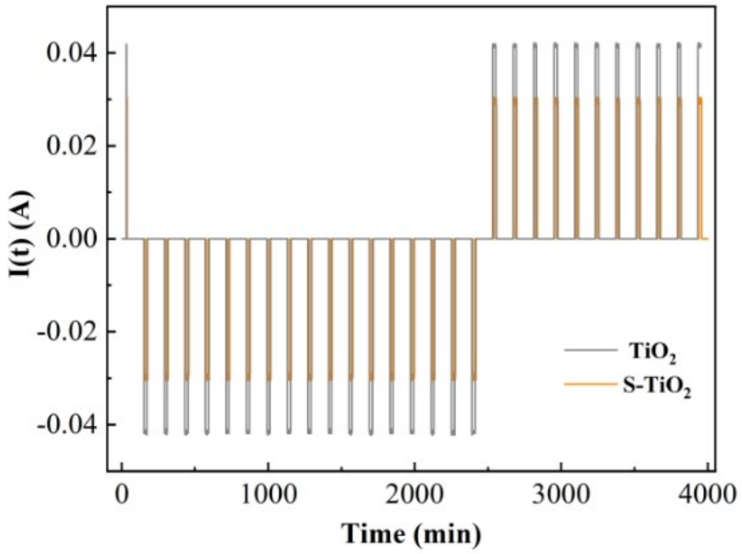

Fig. S4 Diagram of current versus time.

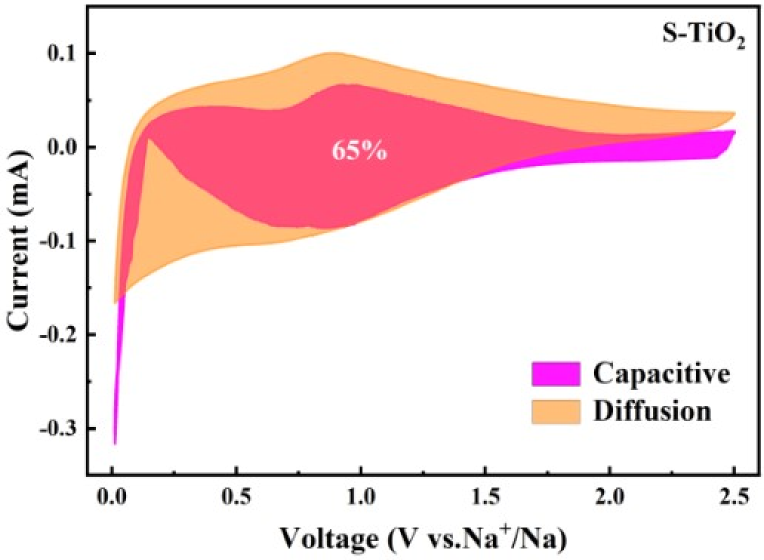

Fig. S5 CV curve with the pseudocapacitive contribution shown by the red region at a scan rate of 0.5 mV s $^{-1}$.